American Mineralogist, Volume 59, pages 280–290, 1974

Contribution to Pegmatite Phosphate Giant Crystal Paragenesis: II. The Crystal Chemistry of Wyllieite, $Na_2Fe^{2+}{}_2Al[PO_4]_3$, A Primary Phase

PAUL BRIAN MOORE, AND JOANN MOLIN-CASE

Department of the Geophysical Sciences, The University of Chicago, Chicago, Illinois 60637[1]

Abstract

Wyllieite, ideally $4Na_2Fe^{2+}{}_2Al[PO_4]_3$, a 11.868(15), b 12.382(12), c 6.354(9), β 114.52°(0.08°), space group $P2_1/n$, is a primary crystallized phase in pegmatites and is structurally related to the alluaudite mineral group. $R(hkl) = 0.092$ for 3200 reflections.

The ordered couple, $Fe^{2+}Al^{3+}$, occurs in the crystal and results in a degradation of the alluaudite symmetry. The structure formula can be written $X(1a)_2X(1b)_2X(2)_4M(1)_4M(2a)_4$ $M(2b)_4[PO_4]_{12}$ with the following approximate site occupancies: $X(1a) = 1.82\ Na^+ + 0.18$ Hole, $X(1b) = 1.0\ Ca^{2+} + 1.0\ Mn^{2+}$, $X(2) = 2.78\ Na^+ + 1.22$ Hole, $M(1) = 3.0\ Fe^{2+} + 1.0\ Mg^{2+}$, $M(2a) = 4.0\ Fe^{2+}$, $M(2b) = 3.0\ Al^{3+} + 1.0\ Fe^{2+}$. The average polyhedral distances are $X(1a)^{[8]}$-O 2.53 Å, $X(1b)^{[6]}$-O 2.21, $X(2)^{[6]}$-O 2.72, $M(1)^{[6]}$-O 2.23, $M(2a)^{[6]}$-O 2.10, $M(2b)^{[6]}$-O 1.97, P(1)-O 1.54, P(2a)-O 1.53, P(2b)-O 1.53. The $X(1)$ polyhedra are distorted cubes, $X(2)$ a distorted square antiprism, $M(1)$ a bifurcated square pyramid, and $M(2)$ are octahedra.

Several crystal-chemical and paragenetic conclusions are drawn: that primary pegmatite phosphates crystallize with the Fe^{2+} valence state, that the wyllieite (alluaudite) structure type is the high temperature dimorph of certain phosphate analogues of the garnet structure type, and that griphite is a metasomatic product. A speculation regarding corrosion of primary alkali ferrous phosphates in pegmatites is based on the hypothetical oxidation reaction $Me^{2+} + (H_2O) \rightarrow Me^{3+} - (OH)^- + H \uparrow$.

Introduction

Complex granite pegmatites often contain significant quantities of accessory minerals such as lithium- and beryllium-bearing silicates, alkali and alkaline-earth transition metal phosphates, and transition metal niobates and tantalates. Such accessory minerals as the transition metal phosphates do not appear to be evenly distributed over a random selection of granite pegmatites but occur within pegmatites derived from a local mutually common source. Thus, variable amounts of primary lithium-bearing phosphates occur throughout the Black Hills and New England pegmatites but are practically absent throughout the pegmatites of the Pikes Peak district in Colorado. Within the broader problem of phosphate and transition metal distributions in a suite of genetically related pegmatites is the problem of the crystal chemistry of these phases. At present, it is incompletely understood, and only through detailed analysis of their atomic arrangements can we hope to evolve a concrete understanding of their crystal chemistry and then proceed to answer questions regarding their occurrence and relationship in and to the pegmatite body.

Wyllieite was recently reported as a new species by Moore and Ito (1973). It was encountered as large, up to 10 cm, interlocking or euhedral crystals embedded in bull quartz, muscovite, perthite, and albitized perthite from the Victory Mine pegmatite, near Custer, South Dakota. On account of the bluish-green color and similar optical properties, it was misidentified as triphylite by Pecora and Fahey (1949). The pegmatite was once accessible by two shafts, but the abandoned excavation is presently flooded; specimens culled on the dump indicate that the mineral was abundant and that it was, at least locally, an important primary phase.

The most significant aspect of wyllieite is its structural relationship to the alluaudite group of minerals. Details of the crystal chemistry of alluaudites, rather common giant phases in certain pegmatites, were recently published by Moore (1971a). Wyllieite, however, differs in six important ways: (1) Wyllieite is a primary phase which grew as

[1] Former address for the junior author.

well-developed euhedral crystals. Alluaudites, on the other hand, are anhedral and nodular in outline with textures suggesting partial to complete metasomatic replacement of triphylite-lithiophilite, heterosite-purpurite, and sicklerite-ferrisicklerite. (2) Wyllieite exhibits only one perfect cleavage, all other cleavage directions poorly developed. Alluaudites show at least two good cleavage directions. (3) Wyllieite crystallizes in space group $P2_1/n$ and is a highly ordered compound whereas alluaudites yield $C2/c$ space group and are extensively disordered. (4) Aluminum is an essential constituent of wyllieite but generally absent in alluaudites. (5) In wyllieite, all alkali and alkaline-earth atomic positions are predominantly occupied, whereas these positions are partially to completely empty in alluaudites. (6) In wyllieite, Fe^{3+} is practically absent while extensive to complete oxidation of Fe^{2+} to Fe^{3+} occurs in alluaudites.

Wyllieite is the first reported alluaudite-like structure which is unambiguously a primary crystallized phase. This observation shall be later advanced as a general argument that iron in the phosphate-rich units of such pegmatites occurred in the divalent state and that all phosphates containing ferric iron are late stage, metasomatically exchanged and/or hydrothermally reworked products of earlier primary phases. To clarify the general crystal chemistry of wyllieite and the alluaudites, we present a detailed crystal chemical analysis of this species.

Experimental

Table 1 compares the unit cell data for wyllieite with those for the Buranga alluaudite, whose crystal structure was analyzed by Moore (1971a). Curiously, the unit cell volume is smaller for the unoxidized alkali-rich wyllieite than for the highly oxidized and extensively leached alluaudite.

For the structure analysis, a transparent nearly equant fragment of wyllieite, measuring about 0.15 mm on an edge, was removed from the type material. Three-dimensional data were collected in a PICKER automated diffractometer with a graphite monochromator. Intensities were measured with Mo$K\alpha$ radiation by scanning 3° (2θ) across each peak with a speed of 2°/minute and a take-off angle of 1.5°. The backgrounds on each side of the scan were each counted for 20 seconds.

Of the 5160 points in reciprocal space (including 3 standard reflections collected for at least every 100 reflections) sampled out to $2\theta = 75°$, 3200 were eventually used in the refinement. Those with $I \leqq 2\sigma$ (I) were not included in the refinement. In addition, 18 other reflections (14 of which showed anomalous background) were removed before the last two cycles of refinement. The measured intensities were corrected for Lorentz and polarization effects. An instrument stability constant of 0.02 was included in the calculation of the standard deviation of the derived structure factor. No absorption correction was applied since scans about selected reflections showed that the intensity distribution was uniform within 5 percent of the mean value.

Solution and Refinement of the Structure

The crystal cell parameters of wyllieite suggested that the structure is closely related to the alluaudite group of minerals. The space group $P2_1/n$ is a subgroup of $C2/c$ and is obtained from the latter by

TABLE 1. Wyllieite. Structure Cell Data

	Wyllieite	Alluaudite (Buranga)*
a(Å)	11.868(15)	12.004(2)
b(Å)	12.382(12)	12.533(4)
c(Å)	6.354(9)	6.404(1)
β	114.52(8)°	114.4(1)°
V(Å^3)	849.5	877.4
space group	$P2_1/n$	C2/c
cell formula	$Na_{5.26}Ca_{0.77}Mg_{0.86}Mn_{1.03}Fe^{2+}_{7.58}Al_{2.96}(P_{11.57},(H_4)_{0.36})O_{46.95}$	$Na_{2.5}Li_{0.1}Ca_{0.5}Mn^{2+}_{4.5}Mg_{0.2}Fe^{3+}_{7.9}[PO_4]_{12.0}$
specific gravity	3.601(3)	3.45
density (gm/cm^3)	3.60	3.62
sum of cations	30.5	27.7
average cation radius	0.58	0.52

*Data of Fisher (1955).

suppressing the inversion center at ¼, ¼, 0, *etc*, and the 2-fold rotor at 0, *y*, ½, *etc*, with no change in cell orientation. Solution of the structure began with the atomic coordinates of Moore (1971a) for alluaudite. The general $M(2)$ octahedral position was split into two general non-equivalent positions, $M(2a)$ and $M(2b)$, for space group $P2_1/n$. Likewise $X(1)$ was split into two special positions at inversion centers. The $M(1)$ and $P(1)$ atoms, formerly on the 2-fold rotor, now became general positions with no symmetry. All remaining atoms in general positions were split into pairs of non-equivalent positions as was done for $M(2)$.

To initiate refinement, it was proposed that the Al^{3+} cations were ordered and that the split $M(2a) = Fe^{2+}$ and $M(2b) = Al^{3+}$. The large alkali positions $X(1a)$ and $X(1b)$ were filled with Na. Position $X(2)$, which is empty in alluaudite, was split into $X(2a)$ and $X(2b)$ and the remaining large alkali atoms were evenly distributed between $X(2a)$ and $X(2b)$. Least squares refinement of the scale factor led to $R(hkl) = \{\Sigma||F(obs)| - |F(calc)||/\Sigma|F(obs)|\} = 0.33$, based on alluaudite coordinates. Site multiplicity refinement for $X(1a)$, $X(1b)$, $X(2a)$, $X(2b)$, $M(2a)$, and $M(2b)$ indicated that $X(1b)$ required electron density heavier than Na^+ and that $X(2a)$ and $X(2b)$ were empty.

At this stage, a difference synthesis revealed that the empty $X(2)$ position proposed by Moore (1971a) to account for excess alkalies in some alluaudite analyses does not accommodate cations.[2] The correct $X(2)$ position proved to be located at *ca* 0, 0, ¼ on the pseudo 2-fold rotor.

After readjustment of site occupancies as suggested by the difference synthesis, convergence was rapid. It was necessary to split $X(1b)$ away from its inversion center on account of the observed density maximum on the difference synthesis. Such a "half-atom" model is not unusual for large alkalies and is similar to problems encountered in structure refinement of the feldspars. Site multiplicity refinement, combined with careful selection of mixed scattering curves and three cycles of atomic coordinate parameter refinement resulted in smooth convergence to $R(hkl) = 0.12$. At this stage, adjustments were made in the choice of mixed scattering curves, and the isotropic thermal vibration parameters of $X(1a)$ and $X(2)$ were fixed at 1.2 Å² (a typical value for Na^+ in an oxygen environment). After two cycles of full-matrix isotropic thermal vibration and atomic coordinate parameter refinement, $R(hkl)$ converged to 0.092 for all 3200 reflections and to 0.056 for the 1300 reflections with intensities above three times the estimated background errors. Refinement utilized a local modification of the ORFLS program for IBM 7094 computers of Busing, Martin, and Levy (1962) and the scattering curves for Na^+, Ca^+, Mg^+, Fe^{2+}, Al^{2+}, P^{3+}, and O^{1-} were obtained from tables in MacGillavry and Rieck (1962). Final atomic coordinates, occupancies, and isotropic thermal vibration parameters appear in Table 2, and the structure factor data are offered in Table 3.[3]

TABLE 2. Wyllieite. Site Occupancies, Atomic Coordinates and Isotropic Thermal Vibration Parameters

	M	x	y	z	B(Å²)
X(1a)	1.82 Na^{1+} + 0.18 Hole	0.5000	0.0000	0.0000	(1.20)
X(1b)	1.0 Ca^{2+} + 1.0 Mn^{2+}	.4903(2)	.0013(2)	.5045(5)	.16(2)
X(2)	2.78 Na^{1+} + 1.22 Hole	-.0004(4)	-.0218(4)	.2485(8)	(1.20)
M(1)	3.0 Fe^{2+} + 1.0 Mg^{2+}	-.0005(1)	.2638(1)	.2366(2)	.78(2)
M(2a)	4.0 Fe^{2+}	.2726(1)	-.3516(1)	.3626(2)	1.09(2)
M(2b)	3.0 Al^{3+} + 1.0 Fe^{2+}	.2187(1)	-.1664(1)	.6434(3)	.60(2)
P(1)	4.0	-.0072(1)	-.2854(1)	.2592(3)	.65(2)
P(2a)	4.0	.2381(1)	-.1143(1)	.1457(3)	.73(2)
P(2b)	4.0	.2376(1)	.0971(1)	.6175(3)	.81(2)
O(1a)	4.0	.4531(4)	-.2889(4)	.5509(8)	1.07(7)
O(1b)	4.0	.4498(4)	-.7170(4)	.0167(8)	.98(6)
O(2a)	4.0	.0820(4)	-.3737(4)	.2429(9)	1.27(7)
O(2b)	4.0	.1104(5)	-.6490(4)	.7199(9)	1.43(8)
O(3a)	4.0	.3432(5)	-.3470(4)	.1114(9)	1.30(7)
O(3b)	4.0	.3189(5)	-.6733(4)	.5866(9)	1.31(8)
O(4a)	4.0	.1219(4)	.4020(4)	.2807(8)	1.10(7)
O(4b)	4.0	.1288(5)	-.4148(4)	.8536(9)	1.36(7)
O(5a)	4.0	.2216(4)	-.1840(4)	.3288(8)	1.20(7)
O(5b)	4.0	.2380(5)	-.8336(4)	.8177(9)	1.31(7)
O(6a)	4.0	.3310(5)	-.5083(4)	.3837(9)	1.54(8)
O(6b)	4.0	.3226(5)	-.5127(4)	.8839(9)	1.64(8)

Discussion of the Structure (P.B.M.)

General Architecture

Excepting the $X(2)$ site, the wyllieite atomic arrangement is topologically identical to that of alluaudite as reported by Moore (1971a). Consequently, it is not necessary to redescribe the general wyllieite structure. The geometrical distinctions, however, are important and shall be explored in detail. In fact, since wyllieite is an extensively ordered phase and has all sites extensively occupied, we are now in a position to propose some general

[2] Since no extra Na^+ was present in the highly oxidized Buranga alluaudite, the final difference synthesis of Moore (1971a) failed to reveal any density and the possible site had to be inferred.

[3] To obtain a copy of Table 3, order NAPS Document 02343 by remitting $1.50 for microfiche (or $5.00 for photocopies up to 30 pages) payable to Microfiche Publications, 305 East 46th Street, New York, N.Y. 10017. Please check the most recent issue of this journal for the current address and prices.

crystal-chemical trends for the entire alluaudite group of minerals.

Ordering Scheme

The $M(2)$ alluaudite position is split into $M(2a)$ and $M(2b)$ in wyllieite, with $M(2b)$ receiving most of the Al^{3+} cations reported in the analysis. $M(2a)$ is primarily occupied by Fe^{2+}. This results in an ordered edge-sharing chain of octahedra (Fig. 1a) in contrast to the disordered chain in alluaudites (Fig. 1b). Since Mg^{2+} and Al^{3+} cannot be distinguished by scattering curves alone, we combined electron density distributions with average interatomic distances to assess site populations.

Extensive order also appears in the alkali-alkaline earth $X(1a)$, $X(1b)$, and $X(2)$ positions. Figure 2 is a sketch of one level of the . . . $X(2)$-$X(2)$ . . . and . . . $X(1a)$-$X(1b)$ . . . polyhedral chains. As in alluaudite, $X(1a)$ and $X(1b)$ are centered in distorted cubes which share faces to form a chain running parallel to the [001] direction. The $X(2)$ cations, incorrectly located in the alluaudite structure, are surrounded by six "inner" and two "outer" oxygen atoms, defining a highly distorted square antiprism. Such antiprisms share edges to form a chain, also running parallel to the [001] direction. Figure 2 also facilitates interpretation of the interatomic distance tables since the non-equivalent atom positions are labelled. The $X(1a)$ site is essentially occupied with Na^{+}. However, $X(1b)$ must contain cations of higher electron density; the best

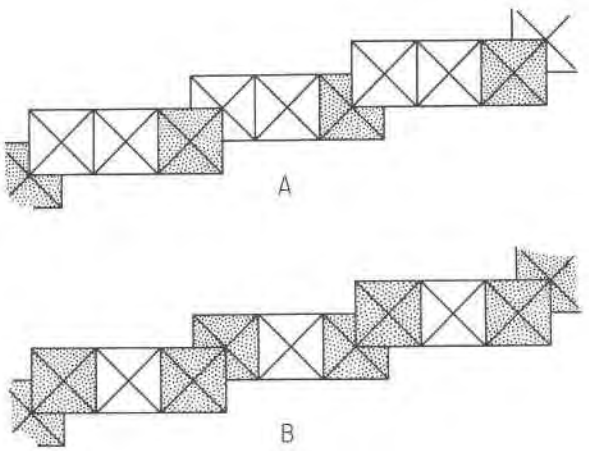

FIG. 1. Ordering of cations in the octahedral chains in (A) wyllieite and (B) alluaudite. M^{3+} sites are stippled, M^{2+} sites are unshaded.

fit, based on electron density and interatomic distances, suggested that $X(1b)$ contains 0.5 Mn^{2+} + 0.5 Ca^{2+}. The $X(2)$ position is not fully occupied, the refinement suggesting an occupancy of 2.7 Na^{+} + 1.3 Hole.

Interatomic Distances

Perhaps the most convincing evidence for extensive ordering of cations in wyllieite are the Me-O interatomic distances which are given in Table 4. The average $M(2b)$-O distance of 1.97 Å indicates a site primarily occupied by Al^{3+} with some Fe^{2+} pres-

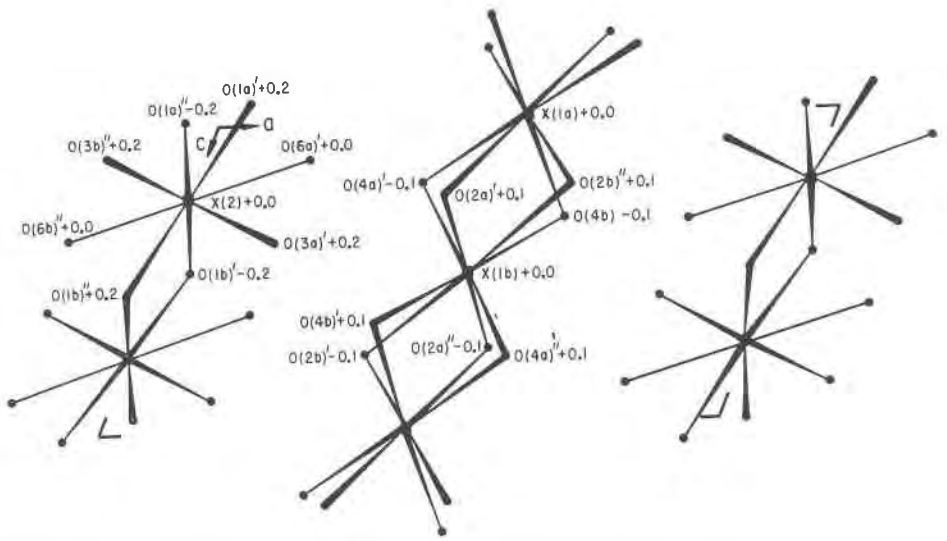

FIG. 2. Spoke diagram of the $X(1)$ and $X(2)$ polyhedra in wyllieite. Heights are as fractional coordinates in y. Atoms are labelled to conform with Table 4.

TABLE 4. Wyllieite. Polyhedral Interatomic Distances*

M(1)			M(2b)			X(1b)			P(1)		
M(1)	-O(1b)″	2.173 Å	M(2b)	-O(2b)′	1.858	X(1b)	-O(2a)′	2.119	P(1)	-O(1a)″	1.517
	-O(4a)	2.185		-O(1b)′	1.933		-O(2a)″	2.148		-O(2b)‴	1.520
	-O(3a)′	2.192		-O(3b)′	1.945					-O(1b)′	1.551
	-O(1a)′	2.221		-O(6b)′	1.955		-O(4a)′	2.136		-O(2a)	1.554
	-O(3b)″	2.250		-O(5a)	2.026		-O(4a)″	2.162			
	-O(4b)‴	2.328		-O(5b)′	2.123					average	1.536
							-O(4b)′	2.224			
	average	2.225 Å		average	1.973		-O(4b)″	2.465	O(2a)	-O(2b)‴	2.409[a]
									O(1b)′	-O(2b)‴	2.452
O(1b)″	-O(3b)″	2.579[b]	O(1b)′	-O(3b)′	2.579[b]		average	2.209	O(1a)″	-O(1b)′	2.501
O(1a)′	-O(3a)′	2.645[b]	O(1b)′	-O(5a)	2.631				O(1a)″	-O(2a)	2.515
O(4a)	-O(4b)‴	2.737[c]	O(2b)′	-O(5b)′	2.668		-O(2b)	3.114	O(1a)″	-O(2b)‴	2.568
O(1b)″	-O(3a)′	2.997	O(1b)′	-O(5b)′	2.714		-O(2b)″	3.285	O(1b)′	-O(2a)	2.592
O(1a)′	-O(4a)	3.043									
O(3b)″	-O(4b)‴	3.046	O(3b)′	-O(6b)′	2.730	2O(2a)′	-O(2b)″	2.409[a,d]		average	2.506
O(4a)	-O(3a)′	3.148	O(2b)′	-O(5a)	2.764[b]	2O(4a)′	-O(4b)″	2.737[c,d]			
O(1a)′	-O(3b)″	3.204	O(5a)	-O(5b)′	2.795[b]	2O(2a)′	-O(4b)′	2.797[d]		P(2a)	
O(1b)″	-O(4b)‴	3.254	O(2b)′	-O(6b)′	2.846	2O(4a)′	-O(2a)′	2.813[d]			
O(3b)″	-O(3a)′	3.666				2O(2b)′	-O(4b)′	3.005[d]	P(2a)	-O(6a)′	1.516
O(1b)″	-O(4a)	3.769	O(3b)′	-O(5b)′	2.861	2O(4a)′	-O(2b)′	3.566		-O(5a)	1.525
O(1a)′	-O(4b)‴	3.801	O(1b)′	-O(6b)′	2.861					-O(3b)′	1.530
			O(2b)′	-O(3b)′	2.944		average	2.888		-O(4a)′	1.542
	average	3.157	O(5a)	-O(6b)′	2.983						
							X(2)			average	1.528
	M(2a)			average	2.783						
						X(2)	-O(6a)′	2.485	2O(6a)′	-O(3b)′	2.451
M(2a)	-O(6a)	2.046		X(1a)			-O(1a)″	2.608	2O(4a)′	-O(5a)	2.479
	-O(2a)	2.082					-O(6b)″	2.614	2O(3b)′	-O(5a)	2.482
	-O(3a)	2.089	2 X(1a)	-O(2b)′	2.357		-O(3a)′	2.753	2O(6a)′	-O(5a)	2.498
	-O(5b)′	2.099	2	-O(4b)′	2.376		-O(1b)′	2.771	2O(4a)′	-O(3b)′	2.519
	-O(1a)	2.121	2	-O(4a)′	2.679		-O(3b)″	3.108	2O(6a)′	-O(4a)′	2.545
	-O(5a)	2.148	2	-O(2a)′	2.719						
							average	2.723		average	2.496
	average	2.098		average	2.533						
							-O(1b)‴	3.581		P(2b)	
O(3a)	-O(1a)	2.645[b]	2 O(2a)′	-O(2b)″	2.409[a,d]		-O(1a)′	3.624			
O(3a)	-O(6a)	2.686	2 O(4a)′	-O(4b)″	2.737[c,d]				P(2b)	-O(4b)′	1.524
O(2a)	-O(5b)′	2.766	2 O(4a)′	-O(2a)′	2.813[d]	O(3a)′	-O(6a)′	2.686		-O(5b)	1.534
O(5b)′	-O(1a)	2.778	2 O(4a)′	-O(2b)′	2.919[d]	O(3b)″	-O(6b)″	2.731		-O(6b)′	1.534
			2 O(2b)′	-O(4b)′	3.005[d]	O(6a)′	-O(1a)″	3.486		-O(3a)′	1.536
O(2a)	-O(5a)	2.792[b]	2 O(2a)′	-O(4b)′	3.720	O(1b)′	-O(6a)′	4.101			
O(5a)	-O(5b)′	2.795[b]								average	1.532
O(1a)	-O(5a)	2.830		average	2.934	O(1a)″	-O(6b)″	4.156			
O(1a)	-O(6a)	3.056				O(6b)″	-O(1b)′	4.240	O(6b)′	-O(3a)′	2.463
						O(1b)′	-O(3a)′	4.855	O(4b)′	-O(5b)	2.474
O(3a)	-O(5a)	3.117				O(1a)″	-O(3b)″	5.054	O(3a)′	-O(5b)	2.492
O(2a)	-O(6a)	3.182							O(6b)′	-O(5b)	2.512
O(5b)′	-O(6a)	3.201							O(4b)′	-O(3a)′	2.530
O(2a)	-O(3a)	3.544							O(6b)′	-O(4b)′	2.536
	average	2.949								average	2.501

*a = P(1) -X(1), X(2) edge; b = M -M′ shared edge; c = M(1) -X(1) edge; d = X(1) -X(1)′ face. ′ = 1/2 -x, 1/2 +y, 1/2 -z; ″ = 1/2 +x, 1/2 -y, 1/2 +z; ‴ = -x, -y, -z referring to coordinates in Table 2. Estimated standard errors: Me-O ± 0.006 Å; O-O′, X(2)-O ± 0.009 Å.

ent. Using the ionic radii in the tables of Shannon and Prewitt (1969), about 20 percent of the Al^{3+} would have to be replaced by Fe^{2+} to raise the distance to the observed average. This is reasonable on the basis of the chemical analysis and the structure refinement. The 2.10 Å average for $M(2a)$-O, combined with the site refinement, suggests predominant occupation by Fe^{2+}. Some Al^{3+} (*ca* 10 percent) may also substitute at this site, accounting for a slightly higher thermal vibration parameter and average distance shorter than Fe^{2+}-O 2.17 Å from Shannon and Prewitt's (1969) tables.

The $M(1)O_6$ polyhedron is a curiously distorted octahedron which, like alluaudite, is similar to a square pyramid with a bifurcated apex. Four of its twelve edges are shared with other polyhedra: O(1b)-O(3b) and O(1a)-O(3a) with the $M(2)$ octahedra and O(4a)-O(4b) with the $X(1)O_8$ distorted cubes. In addition, edge O(3a)-O(3b) is shared with the $X(2)$-O_{6-8} polyhedron which has an $X(2)$-$M(1)$ metal-metal distance of 3.54 Å.

To appreciate the distortions of the $M(1)O_6$ polyhedron, Table 5 affords the O-$M(1)$-O′ interatomic angles. For the ideal octahedron, these angles would be 90.0°, but in alluaudite and wyllieite they range from 72.8° to 119.7°. In addition, pairs of angles which in alluaudite are symmetry equivalent reveal differences up to 9°. Since wyllieite has large, extensively occupied, alkali positions plus Fe^{2+}-Al^{3+} ordering on opposite sides of the $M(1)O_6$ poly-

hedron, its distortion from 2-fold symmetry is pronounced.

The $X(1)O_{6-8}$ polyhedra are highly distorted cubes. In fact, $X(1b)$, which is preferentially occupied by Mn^{2+} and Ca^{2+} on the basis of the refinement, contains an inner coordination shell of six oxygens ranging from 2.12 to 2.46 Å and two more with limits between 3.11 and 3.28 Å. $X(1a)$ more closely approximates a cube with eight oxygen neighbors between 2.36 and 2.72 Å. It is occupied by the large Na^+ cation. The split $X(1b)$ site probably represents an averaged structure due to the mixed (Mn, Ca) occupancy. Faces between these polyhedra are shared to form an infinite chain parallel to the *c*-axis, if the two outer oxygens of $X(1b)$ are included. The edge distances associated with shared faces are short so that the model is essentially an ionic one.

The $X(2)$ polyhedron is even more complicated. It is a highly distorted square antiprism, but like $X(1b)$, two distances are very long, ranging between 3.58 and 3.62 Å. The remaining six distances range between 2.48 and 3.11 Å, yielding an average $X(2)$-O_6 2.72 Å. According to the refinement, this polyhedron is only partly occupied by Na^+.

To assess the electrostatic valence balances, the following coordination numbers were assigned: $P^{[4]}$, $M(2)^{[6]}$, $M(1)^{[6]}$, $X(1a)^{[8]}$, $X(1b)^{[6]}$, $X(2)^{[6]}$. Partial occupancies were included in the calculation in Table 6. The sum deviation based on twelve oxygen atoms is $\Delta\Sigma = -0.15$, which is in good accord with the chosen cation distribution and coordination numbers. Exact neutrality would probably require a weak contribution of the long $X(1b)$-O and $X(2)$-O distances which were excluded from the calculation.

TABLE 5. O–M(1)–O′ Angles in Alluaudite and Wyllieite

	Alluaudite	Wyllieite
O(1a)-M(1)-O(3a)	72.8°	73.6°
O(1b)- " -O(3b)	72.8	71.3
O(4a)- " -O(4b)	75.8	74.6
O(3a)- " -O(4a)	85.3	92.0
O(3b)- " -O(4b)	85.3	83.4
O(1a)- " -O(4a)	88.4	87.4
O(1b)- " -O(4b)	88.4	92.5
O(1a)- " -O(3b)	91.1	91.6
O(1b)- " -O(3a)	91.1	86.7
O(3a)- " -O(3b)'	114.7	111.2
O(1a)- " -O(4b)	115.6	113.3
O(1b)- " -O(4a)	115.6	119.7

Table 1 reveals a curious feature concerning the cell volume of wyllieite and alluaudite. Despite the fact that alluaudite has fewer cations and a smaller average cation radius, it possesses the larger cell. The explanation appears to involve the degree of leaching of the alkalies. In the highly leached alluaudite, the sheet- and chain-like aspect of the alkali-oxygen polyhedra is missing and the potential alkali-oxygen bonds are weak. Alluaudite behaves like sheet silicates in this manner. On the other hand, heterosite-purpurite has a smaller volume than the more reduced triphylite-lithiophilite. In this instance,

TABLE 6. Electrostatic Valence Balances (Σ) for Wyllieite and a Hypothetical Silicate

		Wyllieite[1]		Hypothetical silicate[2]	
			Σ		Σ
O(1a)	P(1)+M(1)+M(2a)+X(2)	5/4+2/6+2/6+1/6(2.78/4)	2.03	4/4+2/6+3/6+2/6	2.16
O(1b)	P(1)+M(1)+M(2b)+X(2)	5/4+2/6+3/6(.75)+2/6(.25)	2.15	4/4+2/6+3/6+2/6	2.16
O(2a)	P(1)+M(2a)+X(1a)+X(1b)	5/4+2/6+1/8(1.82/2)+2/6	2.02	4/4+3/6+2/8+2/6	2.08
O(2b)	P(1)+M(2b)+X(1a)	5/4+3/6(.75)+2/6(.25)+1/8(1.82/2)	1.85	4/4+3/6+2/8	1.75
O(3a)	P(2b)+M(1)+M(2a)+X(2)	5/4+2/6+2/6+1/6(2.78/4)	2.03	4/4+2/6+3/6+2/6	2.16
O(3b)	P(2a)+M(1)+M(2b)+X(2)	5/4+2/6+3/6(.75)+2/6(.25)+1/6(2.78/4)	2.15	4/4+2/6+3/6+2/6	2.16
O(4a)	P(2a)+M(1)+X(1b)+X(1a)	5/4+2/6+2/6+1/8(1.82/2)	2.02	4/4+2/6+2/6+2/8	1.91
O(4b)	P(2b)+M(1)+X(1b)+X(1a)	5/4+2/6+2/6+1/8(1.82/2)	2.02	4/4+2/6+2/6+2/8	1.91
O(5a)	P(2a)+M(2a)+M(2b)	5/4+2/6+3/6(.75)+2/6(.25)	2.03	4/4+3/6+3/6	2.00
O(5b)	P(2b)+M(2a)+M(2b)	5/4+2/6+3/6(.75)+2/6(.25)	2.03	4/4+3/6+3/6	2.00
O(6a)	P(2a)+M(2a)+X(2)	5/4+2/6+1/6(2.78/4)	1.70	4/4+3/6+2/6	1.83
O(6b)	P(2b)+M(2b)+X(2)	5/4+3/6(.75)+2/6(.25)+1/6(2.78/4)	1.82	4/4+3/6+2/6	1.83
		sum	23.85	sum	23.95

1. Based on site distributions in Table 1.
2. For a hypothetical silicate, X(1a) = X(1b) = X(2) = M(1) = charge of 2+; M(2a) = M(2b) = charge of 3+, T = charge of 4+.

these olivine-type structures show a diminution in cell volume which roughly parallels the degree of oxidation of the metals.

The appearance of only one good cleavage in wyllieite, {010}, contrasted with the well-developed {$\bar{1}$01}, {110} and {010} cleavages in alluaudite, corroborates the above arguments. With the presence of many Na-O bonds in wyllieite, the {$\bar{1}$01} and {110} planes would cut the chains of Na-O bonds, and only the {010} direction is parallel to these chains and the MO_6 chains as well.

A Proposed Leaching Sequence and Ordering Scheme

Moore (1971a) has established that alluaudite nodules are sodium-addition metasomatic products of formerly existing triphylites, sicklerites, and heterosites. For the triphylite-lithiophilite series, the progressive leaching of Li^+ and oxidation of the transition metals to produce heterosite is effectively a removal of the Li^+ cation from the $M(1)$ octahedral site in the triphylite (olivine) structure type. This is evident since Eventoff, Martin, and Peacor (1972) established that $M(1)$ is vacant in the refined heterosite structure. Thus, the transition metal atoms in the series are essentially immobile cations.

What is the leaching sequence in the highly complex alluaudite structure? We propose that the cations in the largest sites of alluaudite would be leached first and, as evidence, note that the large $X(1a)$ and $X(2)$ sites are not completely occupied in wyllieite. Thus, the sequence in the direction of decreasing ease of leaching would be $X(2) > X(1a) > X(1b) > M(1) > M(2a) > M(2b)$. But $M(1)$, $M(2a)$, and $M(2b)$, which accommodate the iron atoms in wyllieite, would probably oxidize and remain immobile before their leaching takes place. We suggest that the oxidation sequence would be $M(2a) > M(2b) > M(1)$ by analogy with the refined alluaudite structure of Moore (1971a).

It is also necessary to propose an ideal wyllieite end-member composition. Based on the composition of the crystal in this study, it would be $M(1) = Fe^{2+}$, $M(2a) = Fe^{2+}$, $M(2b) = Al^{3+}$, $X(1b) = Ca^{2+}$, $X(1a) = Na^+$, and $X(2) = \frac{1}{2}\ Na^+ + \frac{1}{2}$ Hole. This leads to $Ca_2Na_4Fe^{2+}{}_8Al^{3+}{}_4[PO_4]_{12} = CaNa_2Fe^{2+}{}_4Al^{3+}{}_2[PO_4]_6$. If Ca is absent, then $X(2)$ must be fully occupied, and the formula reduces to $Na_2Fe^{2+}{}_2Al[PO_4]_3$. Of course, the number of possible end compositions is large since $M(1) = Fe^{2+}$, Mn^{2+}, Mg^{2+}; $M(2b) = Al^{3+}$, Fe^{3+}; $M(2a) = Fe^{2+}$, Mn^{2+}, Fe^{3+} (by analogy with alluaudites); $X(1b) = Ca^{2+}$, Mn^{2+}, Na^+; $X(1a) = Na^+$, Hole; and $X(2) = Na^+$, Hole. Other cations such as Sc^{3+}, Sr^{2+}, Zn^{2+}, *etc*, may also be included. So we conclude that the wyllieite (and alluaudite) structure type may be a basis for a large variety of compounds akin in composition to the alkali phosphate equivalents of the garnet structure type.

The distinction between wyllieites and alluaudites may vanish for certain compositions of primary phases. For example, the primary phase composition $NaCaM^{2+}{}_2M^{2+}[PO_4]_3$ (such as $NaCaFe^{2+}{}_3[PO_4]_3$, where $M(1) = M(2a) = M(2b) = Fe^{2+}$; $X(1b) = Ca^{2+}$; $X(1a) = Ca^{2+}$, and $X(2) = Na^+$) would allow the presence of an additional inversion center at ¼, ¼, 0, *etc*, and the super group $C2/c$. There appears to be no obvious structural reason why distortion to lower symmetry would occur for such a composition. Rather, it would appear that the reduction of alluaudite symmetry to $P2_1/n$ is a result of the $M(2a)$ $M(2b) = M^{2+}M^{3+}$ ordered couple and the consequent distortion of the other polyhedra.

Possibility of Silicate Analogues and Relations with Garnets

Can a silicate analogue exist which is dimorphous to the garnet structure type? We note that the charge balance greatly restricts the admissible compositions. Possibilities include $X(2) = X(1a) = X(1b) = M(1) = Me^{2+}$; $M(2a) = M(2b) = Me^{3+}$; $T = Si^{4+}$, with appropriate selection of cations to fill crystal radii criteria. Computation of electrostatic valence balances for such formulas, using the coordination numbers proposed in this study, reveals no severe deviations and shows that the valence sum is essentially a balanced system. We would propose a composition like $X(2) = Ba^{2+}$, $X(1a) = X(1b) = Ca^{2+}$, $M(1) = Mg^{2+}$, $M(2a) = M(2b) = Fe^{3+}$ resulting in $BaCaMg^{2+}Fe^{3+}{}_2[SiO_4]_3$. Naturally, a large number of possibilities can be suggested, tempered by charge balance and crystal radii conditions; this possible composition seems to possess those desired advantages.

Nature, in fact, has provided an example of a garnet-alluaudite structure type relation in berzeliite-caryinite. In Table 7, we draw attention to two analyses of a manganberzeliite and of caryinite, as found in Landergren (1930) and Boström (1957) respectively. The formula for manganberzeliite is written $(Ca,Na)_3(Mn,Mg,Fe)_2[AsO_4]_3$ analogous to the garnet structure, and caryinite is written (Na,

$Ca,Pb)_2Ca(Mn,Mg)_2[AsO_4]_3$, analogous to the alluaudites. The similarity in composition between the two is striking, the only great difference being the presence of major Pb^{2+} in the caryinite with correspondingly less Ca^{2+}. Caryinite, according to Boström, has space group $P2_1/c$, which is the subgroup of the I-cell orientation of alluaudites to which Strunz (1960) proposed caryinite as isostructural. Transformation of the caryinite cell leads to the $P2_1/n$ orientation of wyllieite. In fact, caryinite is more properly isostructural with wyllieite and probably exhibits a high degree of order. To compare caryinite, berzeliite, griphite, and wyllieite, the following ordering scheme was selected: in the order of ionic radii $M(2b) < M(2a) < M(1) < X(1b) < X(1a) < X(2)$, cations were placed, first those with smallest ionic radius and so on until a deficiency or excess occurred in $X(2)$. Atomic population computations of the chemical analyses of these minerals (Table 7) were based on oxygen = 48. Table 8 provides the ordering scheme based on cation distributions according to their increasing ionic radii for these four species. The $X(1a)$ and $X(1b)$ sites in caryinite are spatially similar to the distorted cube in the garnet-structure berzeliite. But $X(2)$ is even larger than the distorted cube of the garnet structure and apparently accommodates the large Pb^{2+} and K^+ cations which are absent in berzeliite.

Sjögren (1875) and Lindgren (1881) have observed at Långban, Sweden, that berzeliites invariably rim and replace caryinites. In all likelihood, berzeliite is a metasomatic exchange product where highly mobile Pb^{2+} was removed and Ca^{2+} added, suggesting that caryinites predate berzeliites.

TABLE 7. Total Cations Based on Oxygen = 48 for Caryinite, Manganberzeliite, Griphite, and Wyllieite

	Caryinite[1]	Berzeliite[2]	Griphite[3]	Wyllieite[4]
$(H_4)^{4+}$	0.39	0.30	2.21	0.39
		} 11.98		
As^{5+}	11.37	11.68	-	-
	} 11.92		} 12.27	} 12.21
P^{5+}	0.07	-	10.06	11.82
Si^{4+}	0.09	-	-	-
Fe^{3+}	-	-	-	-
Al^{3+}	-	-	3.69	3.02
Mg^{2+}	2.02	1.16	-	0.88
Fe^{2+}	0.20	0.30	1.04	7.75
Mn^{2+}	6.93	6.55	7.74	1.05
Na^{1+}	4.39	3.38	3.30	5.38
K^{1+}	0.21	-	-	-
Ca^{2+}	5.70	8.47	2.46	0.79
Ba^{2+}	0.18	-	-	-
Pb^{2+}	1.09	-	-	-

1. From analysis in Boström (1957).
2. Do., Landergren (1930).
3. Do., McConnell (1942).
4. Do., Moore and Ito (1973).

Griphite is related to garnet in its structure according to McConnell (1942). Peacor and Simmons (1972) confirmed McConnell's cubic cell, but their study revealed a space group of lower symmetry. Casting the Headden analysis in McConnell (1942) into a site preference scheme allied to wyllieite, we obtain (based on 48 oxygens) the results in Tables

TABLE 8. Hypothetical Site Distributions (Oxygen = 48) for Caryinite, Berzeliite, Griphite, Wyllieite, Based on Increasing Ionic Size

	Caryinite	Berzeliite	Griphite	Wyllieite
X(1a)	$Na^+_{1.87}Ca^{2+}_{0.13}$	$Ca^{2+}_{2.00}$	$Na^+_{1.07}Ca^{2+}_{0.93}$	$Na^+_{2.00}$
X(1b)	$Ca^{2+}_{2.00}$	$Ca^{2+}_{2.00}$	$Ca^{2+}_{1.53}Mn^{2+}_{0.47}$	$Ca^{2+}_{0.79}Mn^{2+}_{0.70}Na^+_{0.51}$
X(2)	$Na^+_{2.52}Pb^{2+}_{1.09}K^+_{0.21}Ba^{2+}_{0.18}$	$Na^+_{3.38}Ca^{2+}_{0.48}Hole_{0.14}$	$Na^+_{2.23}Hole_{1.77}$	$Na^+_{2.87}Hole_{1.13}$
M(1)	$Ca^{2+}_{3.57}Mn^{2+}_{0.43}$	$Ca^{2+}_{3.99}Mn^{2+}_{0.01}$	$Mn^{2+}_{4.00}$	$Fe^{2+}_{3.65}Mn^{2+}_{0.35}$
M(2a)	$Mn^{2+}_{4.00}$	$Mn^{2+}_{4.00}$	$Mn^{2+}_{3.27}Fe^{2+}_{0.73}$	$Fe^{2+}_{4.00}$
M(2b)	$Mg^{2+}_{2.02}Mn^{2+}_{1.78}Fe^{2+}_{0.20}$	$Mn^{2+}_{2.54}Mg^{2+}_{1.16}Fe^{2+}_{0.30}$	$Al^{3+}_{3.69}Fe^{2+}_{0.31}$	$Al^{3+}_{3.02}Mg^{2+}_{0.88}Fe^{2+}_{0.10}$
excess*	$Mn^{2+}_{0.72}$			

*Mn^{2+} was arbitrarily chosen as the excess.

7 and 8. Note that the distribution of cations solely based on the chemical analysis and ionic size for wyllieite in Table 8 is not greatly different from the proposed distribution scheme in Table 2 based on least-squares refinement and interatomic distances. Distribution and composition are very similar to those of wyllieite, the griphite differing only in containing predominant Mn^{2+} over Fe^{2+}, more Ca^{2+} and less Na^{+}. Griphite always occurs as nodular masses which are often fractured and healed by fillings of apatite. Griphite analyses show variable amounts of Fe/(Fe+Mn) but their Al^{3+} contents do not vary greatly. In addition, significant water (as hydroxyl groups) and fluorine are present. These observations lend well to the proposition that griphite is a metasomatic product of some pre-existing phase in much the same way that alluaudites are metasomatic products of the triphylite-lithiophilite, ferrisicklerite-sicklerite, and heterosite-purpurite series. By analogy with berzeliite and caryinite we suggest that the pre-existing phase belonged to the wyllieite structure type.

Heating Experiments

Wyllieite and griphite were powdered and each submitted to heating at 750°C for 40 hours in open tubes and in sealed silica tubes, the products being then quenched in ice water. The results appear as a composite of powder photographs in Figure 3. Figures 3a and 3b are photographs of griphite and wyllieite respectively. Figure 3c is of wyllieite heated *in vacuo*. It is clearly the disordered equivalent of wyllieite since the closely spaced sharp lines of medium to weak intensity become diffuse and weak, comparable with photographs of alluaudites. The product is a deep greenish-black color which probably results from mixed valence electron transfer between Fe^{2+} and the minor Fe^{3+} distributed over the disordered octahedral chains. Wyllieite heated in air breaks down into a mixture which affords a disordered alluaudite patterns (Fig. 3d) with subsidiary hematite.

Griphite, on the other hand, breaks down into several products *in vacuo*. The silica tube was observed to contain at least two discrete phases: a pale yel-

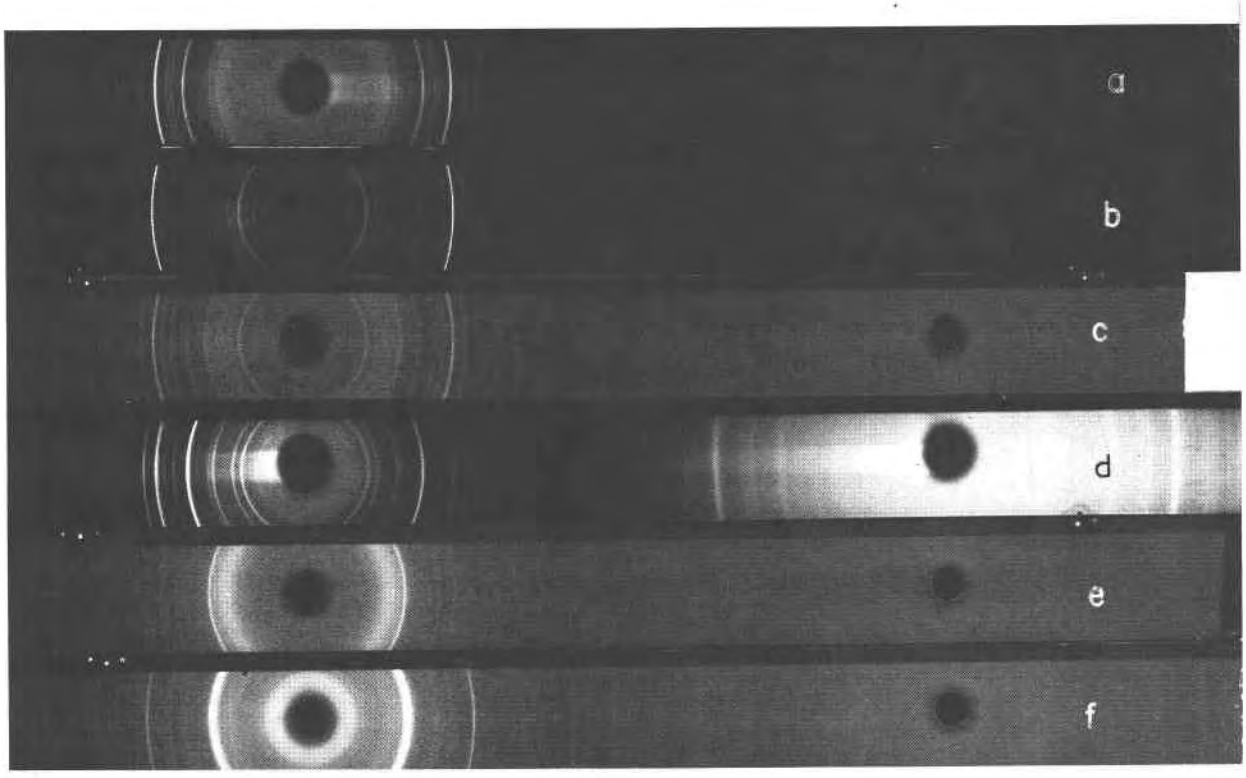

FIG. 3, a-f. Powder patterns of wyllieite, related phases and breakdown products. 114.6 mm camera diameter, Fe/Mn radiation. a. Griphite from Sitting Bull pegmatite. b. Wyllieite. c. Wyllieite heated *in vacuo* to 750°C and quenched. d. Wyllieite heated in air to 750°C and quenched. e. Yellow fraction of griphite heated *in vacuo* at 750°C and quenched. f. White product found with e.

low product, and a colorless crystalline sublimate along the walls of the tube. In addition, the walls of the tube were frosted, and small water drops were noted. Powder photographs of these two materials appear in Figures 3e and 3f. Powder patterns of the colorless product correspond well with $Al[PO_4]$. The yellow phase suggests relationship with the $BaMg_2[PO_4]_2$ phase of Hoffman (1963). Writing the griphite formula on the basis of 48 oxygen atoms in the cell, we have $Na_{3.30}Ca_{2.46}Mn^{2+}_{7.75}Fe^{2+}_{1.04}Al_{3.69}P_{10.06}(H_4)_{2.21}O_{48}$. A balanced breakdown might be $3.69\ Al[PO_4] + 3.18[(Ca_{0.77}Mn_{0.23})Mn_{2.00}[PO_4]_2] + (3.30\ NaOH + 2.77\ H_2O + 1.04\ FeO + 0.65\ MnO)$. The remainder, in parentheses, are the inferred components of the undetermined products. Etching of the tube walls and water droplets are taken as evidence for the appearance of reaction volatiles and the appearance of corrosive alkali hydroxide. The griphite decomposition *in vacuo* is interpreted, thus, as the products $Al[PO_4] + BaMg_2[PO_4]_2$ structure type and volatiles.

Some Conclusions on Wyllieite-Alluaudite Parageneses

Because of the inherent complexity of the wyllieite chemistry, we at first looked back and wondered if the structure analysis was worth all the effort put into it. However, our knowledge of phosphate crystal chemistry has advanced to the level that definite conclusions can now be drawn, and some of these conclusions are of considerable importance to pegmatite genesis. The senior author advances the following statements, based on this study and on his earlier studies on primary transition metal phosphate phases.

1. Since no detailed phase equilibria studies have been done on any of these systems, the difficult route of crystal structure analysis was necessary in the interpretation of the primary phosphate parageneses. It is now seriously doubted whether any rational statements can be made about parageneses and pegmatite genesis without foreknowledge of the crystal chemistry of the phases since metasomatic processes can be described from several routes, many of which are not crystallochemically sensible.
2. Wyllieite is the parent primary phase and alluaudites are either alkali-leached oxidation products of this phase or (Na,Ca)-metasomatic exchange products of the triphylite-lithiophilite series and its series of leached products. It is proposed that alluaudites with broad cleavage surfaces may, in fact, have been derived from wyllieites just as ferrisicklerite and heterosite have been derived from triphylites. It is noted that such alluaudites are cloudy and turbid even in small fragments whereas primary wyllieite is holocrystalline and glassy-clear in appearance.
3. The wyllieite (and alluaudite) structure type is a possible dimorph or pseudo-dimorph of the garnet structure type, *i.e.*, suitable compositions may take on either structure under appropriate conditions. Accepting this argument, the berzeliite-caryinite and the wyllieite-griphite parageneses are consistent with the crystal chemical evidence. The qualifier 'pseudo-dimorph' is used since additional larger cations may be necessary to stabilize the wyllieite structure with its square antiprism site, $X(2)$. If not, then it is possible that some garnet composition silicates may exist with the wyllieite structure.
4. The breakdown of griphite into several products may indicate that extensive hydroxylation may inhibit its inversion to the wyllieite structure. It appears that more studies on griphite compositions are needed to better clarify this complex problem. It is also possible that the $BaMg_2[PO_4]_2$ structure type may eventually be found as a primary phosphate phase.

The following statements have direct bearing on pegmatite genesis.

5. All primary transition metal phosphates appear to possess Fe^{2+} as the stable valence state. There is no concrete evidence that any primary phosphate has crystallized from a pegmatite with Fe^{3+} as the major valence state. Since transition metal phosphates are far more reactive and susceptible to oxidation than transition metal-bearing silicates such as tourmaline, the oxygen fugacity in pegmatites must be very low, at least during the pegmatite's consolidation.
6. With the availability of $[PO_4]^{3-}$ and transition metals, Li-rich pegmatites provide the triphylite-lithiophilite series; Na-rich pegmatites provide the wyllieite and the dickinsonite-arrojadite series; and Ca-rich pegmatites provide the graftonite-beusite series and sarcopside.

Finally, speculation, which follows, is potentially testable. Although evidence is wanting for the existence of such a reaction, it is appealing since no external sources for oxygen or water need be involved for the oxidative and metasomatic processes at later stages. This reaction was advanced by Moore (1971b) to explain thermally dependent intracrystalline autooxidation-reduction reactions involving divalent transition metals and water ligands.

7. Consider the solid state reaction $Me^{2+} + (H_2O) \rightarrow Me^{3+} + (OH)^- + H\uparrow$ and assume that it operates only above some temperature T_0. Crystal-chemically, T_0 is the temperature below which a water molecule will bond to a metal as a ligand in its inner coordination sphere and result in a stable crystal. The autooxidation-reduction model would admit that electronic exchange can only occur when metal and potential water ligand are actually bonded together at some temperature higher than T_0, when the reaction spontaneously proceeds to form hydroxyl-bonded higher valence states of the metal.

This mechanism does not require the addition of external oxygen or the addition of external water because the reaction is an autometasomatic one. Its appealing qualities explain the frequency of ferrisicklerite-heterosite cannibalization of triphylite and the occurrence of alluaudites, in short the common corrosions of primary divalent phosphate species. The degree of corrosion depends on the amount of aqueous rest liquid above T_0. If aqueous rest liquid remains in contact with the primary phosphate below T_0, then the primary phosphate is replaced by hydrated phases such as ludlamite and vivianite. If no aqueous medium remains, then the primary phases appear unoxidized and fresh. The degree of corrosion or hydration of primary giant crystals would provide an estimate of the amount of residual aqueous medium of a pegmatite. Based on the stability of $Fe^{2+}-H_2O$ bonds inferred from the crystal structures of secondary phases and their stabilities, T_0 (if such a temperature does exist) would be in the region of 250-300°C.

Finally, these reactions suggest that the primary phase cannot be inferred through closed-tube heating experiments upon the metasomatic products. This is because such an experiment does not imply reversibility since during the oxidation reactions in the pegmatite, H_2 was removed from the system. In addition, hydroxylation of the metasomatic products may lead to decomposition into phases not encountered for anhydrous starting material.

Acknowledgments

This study was supported by the NSF grant GA-10932-A-1 awarded to the senior author and an MRL grant (NSF) award to The University of Chicago.

References

BOSTRÖM, K. (1957) The chemical composition and symmetry of caryinite. *Ark. Mineral. Geol.* **2,** 333–336.

BUSING, W. R., K. O. MARTIN, AND H. A. LEVY (1962) ORFLS, a Fortran crystallographic least-squares program. *U.S. Nat. Tech. Inform. Serv.* Rep. ORNL-TM-**305.**

EVENTOFF, W., R. MARTIN, AND D. R. PEACOR (1972) The crystal structure of heterosite. *Am. Mineral.* **57,** 45–51.

FISHER, D. J. (1955) Alluaudite. *Am. Mineral.* **40,** 1100–1109.

HOFFMAN, M. V. (1963) The systems BaO–MgO–P_2O_5 and BaO–ZnO–P_2O_5: compounds and fluorescence. *J. Electrochem. Soc.* **110,** 1223–1227.

LANDERGREN, S. (1930) Studier över berzeliitgruppens mineral. *Geol. Fören. Förhandl.* **52,** 123–133.

LINDGREN, W. (1881) Om arseniaterna från Långban. *Geol. Fören. Förhandl.* **5,** 552–558.

MACGILLAVRY, C. H., AND G. D. RIECK (1962) *International Tables for X-ray Crystallography, Vol.* **3.** The Kynoch Press, Birmingham, England.

MCCONNELL, D. (1942) Griphite, a hydrophosphate garnetoid. *Am. Mineral.* **27,** 452–461.

MOORE, P. B. (1971a) Crystal chemistry of the alluaudite structure type: contribution to the paragenesis of pegmatite phosphate giant crystals. *Am. Mineral.* **56,** 1955–1975.

——— (1971b) The $Fe^{2+}_3(H_2O)_n(PO_4)_2$ homologous series: crystal-chemical relationships and oxidized equivalents. *Am. Mineral.* **56,** 1–17.

———, AND J. ITO (1973) Wyllieite, $Na_2Fe_2Al[PO_4]_3$, a new species. *Mineral. Rec.* **4,** 131–136.

PEACOR, D. R., AND W. B. SIMMONS, JR. (1972) New data on griphite. *Am. Mineral.* **57,** 269–272.

PECORA, W. T., AND J. J. FAHEY (1949) Scorzalite from South Dakota: a new occurrence. *Amer. Mineral.* **34,** 685–687.

SHANNON, R. D., AND C. T. PREWITT (1969) Effective ionic radii in oxides and fluorides. *Acta Crystallogr.* **B 25,** 925–946.

SJÖGREN, A. (1875) Mineralogiska notiser. II. Några observationer vid Berzeliitens och Karyinitens förekomst. *Geol. Fören. Förhandl.* **2,** 533–535.

STRUNZ, H. (1960) Karyinit, ein Arsenat vom Strukturtypus der Phosphate Hagendorfit und Alluaudit. *Neues Jahrb. Mineral. Monatsh.* **1960,** 7–15.

Manuscript received, July 16, 1973; accepted for publication, November 16, 1973.